observed in these cobalt(III) complexes. This is consistent with the fact that the 2p peaks in the X-ray photoelectron spectra of cobalt(III) complexes are rarely accompanied by shake-up satellite peaks.[14]

Comparison of CoL_6 Spectra. No common characteristic features of the XANES spectra are found for CoL_6 complexes, except that the main absorption peaks are found around 7730 eV for all the complexes examined. According to the MO calculations, these absorption bands are assigned to the transition from Co 1s orbital to an MO with a Co p orbital as a main component. This means that the 1s–4p orbital energy difference remains almost the same for all the trivalent cobalt complexes examined.

Absorption in the range from the 1s–3d to the 1s–4p transition significantly changes among these complexes. Several intense absorption bands near the edge are found for $[Co(dtc)_3]$ but not for $K_3[Co(CN)_6]$. The dtc ligand has unoccupied MO's to be mixed with the Co 4p orbital. On the other hand, the CN^- ligand has only one unoccupied orbital, 6σ, which can strongly interact with the Co 4p orbital. The absorption near the edge is correlated with unoccupied orbitals of the ligand in cobalt complexes. These suggest that the nature of the ligands reflects on the absorptions before the main peaks.

Isomer Effect. In order to study the relationship between the XANES spectrum and the symmetry around the cobalt ion, the XANES spectra for *cis*- and *trans*-$[CoCl_2(en)_2]NO_3$ (en = 1,2-diaminoethane), for *mer*- and *fac*-$[Co(gly)_3]$ (gly = glycinate ion), and for the F_1, F_2 and F_3 isomers of $[Co(methio)_2]Br$ (methio = L-methionate ion) are compared in Figure 4a–c. The general features of the XANES spectra are similar between isomers.

Spectra of *cis*- and *trans*-$[CoCl_2(en)_2]NO_3$ show differences in the shoulder on the higher energy side; for the trans complex, the shoulder is so pronounced as to become a third peak. On the other hand, the 1s–3d peak is higher for the cis than for the trans complex in agreement with the group-theoretical consideration that this transition is less strictly forbidden in the cis complex with a lower symmetry of C_{2v} as compared with the quasi-D_{2h} symmetry of the trans complex.

Figure 4c shows the XANES spectra of $[Co(methio)_2]Br$ isomers in which methioninate ions are coordinated with the cobalt ion at sulfur, oxygen, and nitrogen atoms. The spectra show differences at the high-energy side of the main peak; isomer F_1, which has two S atoms at trans positions to each other, has a spectrum with two peaks at the high-energy shoulder, whereas the spectra of F_2 and F_3, which have the S atoms at cis positions, show one broad peak at the shoulder. The spectral features of the isomers are parallel to those of $[CoCl_2(en)_2]NO_3$ isomers, considering that O and N as ligators are located near to each other in the spectrochemical series but S is far apart from them.

These examples show that XANES spectra reflect, though not always sensitively, the structure around the absorbing atom.

Conclusions

A systematic study of XANES spectra has been carried out for a series of cobalt(III) complexes. This led to the following conclusions.

(1) The counterion effect has been observed in the XANES spectra of $[Co(NH_3)_6]X_3$ (X = Cl, Br, and I) in their higher energy region, demonstrating that the XANES spectra can exhibit the effect of distant environment which EXAFS cannot show.

(2) The trend of the 1s–3d transition energies is $dtc^- < ox^{2-} < NO_2^- <$ phen $< NH_3$, en $< CN^-$, which roughly corresponds to the spectrochemical series.

(3) According to MO calculations for $[Co(CN)_6]^{3-}$ and $[Co(NO_2)_6]^{3-}$, the main absorption bands can be interpreted as transitions from Co 1s to MO's resulting from the interaction of Co 4p with ligand σ antibonding orbitals.

(4) The general features of XANES spectra differ only slightly between geometrical isomers; however, the XANES spectra appreciably differ between isomers when coordinating atoms considerably differ in their spectrochemical properties.

(5) These findings show that XANES contains very important information on the electronic and geometrical structures around the absorbing atom. Further systematic studies of XANES spectra on series of complexes will establish a general rule.

Acknowledgment. I thank Prof. Hideo Yamatera for his useful discussion and his encouragement. I also thank Prof. Hirohiko Adachi for his advice on the molecular orbital calculations. This work has been performed under the approval of the Photon Factory Program Advisory Committee (Proposal No. 86015).

(13) Bair, R. A.; Goddard, W. A., III. *Phys. Rev. B: Condens. Matter* **1980**, *22*, 2767–2776.
(14) Frost, D. C.; McDowell, C. A.; Woolsey, I. S. *Mol. Phys.* **1974**, *27*, 1473–1489.

Contribution from the Department of Chemistry, The University of Calgary, Calgary, Alberta, Canada T2N 1N4

Silicon-29 NMR Studies of Aqueous Silicate Solutions. 1. Chemical Shifts and Equilibria

Stephen D. Kinrade† and Thomas W. Swaddle*

Received November 25, 1987

In the ^{29}Si NMR spectra of aqueous alkali-metal (M) silicate solutions ($[MOH]:[Si^{IV}] = 1.0$ or higher), variations in solution composition cause displacements of the peaks of up to 1 ppm, largely through interaction of silicate units with M^+. The analysis of the chemical shift data provides a means of predicting ^{29}Si resonance frequencies for new silicate species and has aided in the identification of the $Si_4O_{10}^{4-}$ (Q^3_4) anion, in which the Si atoms are at the corners of a regular tetrahedron. A quantitative study of the dependence of silicate connectivity upon temperature (−5 to +144 °C) and solution composition shows that silicate polymerization is favored by low temperature, low alkalinity, and high $[Si^{IV}]$. In no case could silicate centers with 4-fold connectivity (Q^4) be detected. The effect of M^+ on the distributions of silicate species is small, but the larger M^+ atoms do preferentially stabilize the more highly polymerized silicate anions.

Introduction

The characterization ("speciation") of dissolved silicates in aqueous fluids has long presented a major problem in various geological and technological contexts. Potentiometric studies, in which pH values rather than actual silicate concentrations were measured, have shown that polymerization of aqueous silicates is important and is favored by low temperatures, high Si concentration, and low alkalinity.[1] Raman spectra of aqueous silicate solutions are not very well-defined but suggest that the observed distribution of silicate species is independent of both the solution

†Present address: Department of Chemistry, Lakehead University, Thunder Bay, Ontario, Canada P7B 5E1.

(1) Busey, R. H.; Mesmer, R. E. *Inorg. Chem.* **1977**, *16*, 2444.

0020-1669/88/1327-4253$01.50/0

history[2] and the alkali-metal cation (M^+) used.[3] Although useful information can be obtained from trimethylsilylation studies,[4-9] it is possible that the technique itself may perturb labile equilibria involving the silicate oligomers present in aqueous solution, and the reliable identification of the individual aqueous silicate species in situ has become feasible only through high-resolution ^{29}Si Fourier transform NMR spectroscopy.[10-14] With this technique, Harris and Knight[14] identified 12 silicate structures and made tentative assignments for another six.

The primary objective of the present study was to assess the value of ^{29}Si FT-NMR for the accurate speciation and quantitation of hydrothermal (i.e., high-temperature aqueous) silicate solutions. It transpired that detailed structural information of the kind reported by Harris and Knight[14] is unobtainable at elevated temperatures because of severe line broadening due to Si–Si chemical exchange at rates within the NMR time frame,[15-17] but conversely, the line broadening gives information on the kinetics and mechanism of the exchange process, and this is the topic of a complementary paper.[18]

The ^{29}Si resonances observable at near-ambient temperatures, which cover some 30 ppm, are generally shifted to higher frequencies as the $M^+:Si^{IV}$ ratio[19] is raised (presumably because of deprotonation of the silicate oligomers),[14,20,21] and there is evidence that the resonance frequencies vary with sample dilution,[14] but no systematic study of the effects of solution conditions on ^{29}Si shielding in aqueous silicates has been reported. The present paper addresses this point and shows how such information can be used in identifying new silicate species as well as in providing the necessary background to the calculation of relative concentrations of silicate species from integrated NMR peak areas. This last procedure also requires that the ^{29}Si magnetization be known to decay sufficiently between pulses, and accordingly a study of ^{29}Si longitudinal relaxation times (T_1) in aqueous silicates was completed first.[22]

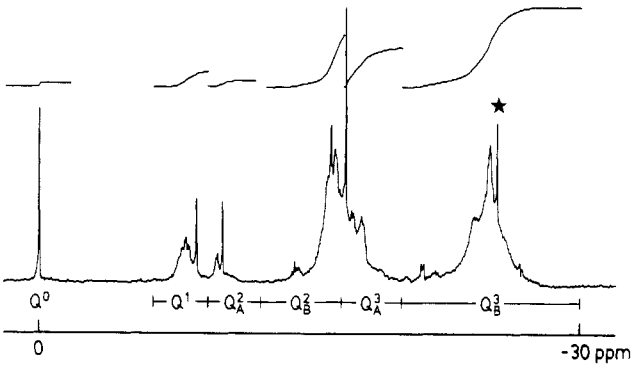

Figure 1. ^{29}Si NMR spectrum, showing band nomenclature and integrations, at 3.3 °C with 1.20 mol kg^{-1} Si and $Na^+:Si^{IV}$ = 1.0:1 (sample 36, 95% ^{29}Si enriched; acquisition time 3 s; delay 72 s; 600 acquisitions; artificial line broadening 1.0 Hz). The star marks the resonance (line 43 of ref 14) assigned in this paper to $Si_4O_{10}^{4-}$.

Experimental Section

Sample Preparation. Deionized distilled water was used throughout these experiments. All labware was cleaned, soaked for 12 h in hot Na_2H_2EDTA solution (2 mmol L^{-1}), and rinsed thoroughly with water.

Amorphous silica was prepared by dropwise hydrolysis of fractionally redistilled silicon tetrachloride (Fisher, technical) in water. The resulting gel was dried at 110 °C, crushed, and washed repeatedly with water (to neutrality of the washings). In addition, two samples of 95.1% ^{29}Si-enriched silica (A, 228 mg; B, 210 mg) were purchased from U.S. Services Inc.; spectrochemical analysis supplied with batch B showed Na, Mg, and Ti to be present in trace amounts (<0.01%), while 52 other elements were undetectable.

Alkali-metal hydroxide solutions were prepared inside screw-capped polyethylene bottles by dissolving solid NaOH or KOH (both Fisher ACS Certified) or RbOH (ICN Pharmaceuticals) in freshly boiled H_2O and D_2O (Bio-Rad, 99.75%) and standardized with potassium hydrogen phthalate. To ensure a strong internal lock signal, solutions were generally made with at least 75% enrichment in ^2H.

Silicate solutions were prepared directly in Teflon-FEP NMR tube liners by dissolving a known quantity of silica, which had been dried at 250 °C, in a weighed portion of MOH solution at 100 °C for 1 h. The silica made from $SiCl_4$ dissolved readily and completely in all solutions except those with $M^+:Si^{IV}$ significantly less than unity. The enriched-silica samples, however, dissolved only slowly and incompletely; the small amounts of undissolved material were apparently crystalline silica, since high purity was claimed by the manufacturer. A fine white powder, representing 8% of batch B of enriched silica, was centrifuged from its solution when first prepared, and further small amounts of a fine white suspension appeared in subsequent dilutions; Harris and co-workers reported similar experiences with enriched silica.[13]

Solutions were contained in Teflon-FEP NMR tube liners in a specially constructed silicon-free pressurizable sample vessel.[23] The samples were pressurized to 1 MPa with nitrogen. Most samples that were also used for T_1 measurements[22] were purged of oxygen with nitrogen.

NMR Measurements. Silicon-29 spectra of 42 different solutions were obtained at 39.75 MHz on a Varian XL-200 spectrometer using 10- and 16-mm probeheads and, for one sample, at 59.61 MHz on a Nicolet 300 spectrometer with a 12-mm probehead as well. The ^{29}Si 90° pulse width, nominally 44 and 49 μs for the Varian 10- and 16-mm probes and 40 μs for the Nicolet, was determined at the beginning of each operating session by using hexamethyldisiloxane. Spectra were generally recorded over a range of temperatures from about −5 to +150 °C.

Glass coil supports gave rise to a broad ^{29}Si background signal centered around −40 ppm relative to the orthosilicate resonance. They were therefore replaced in the 16-mm probehead with equivalent parts machined from Vespel SP-1 resin, and the coils were reattached with Powerbond 920 (Permabond Corp.), a silicon-free, high-temperature-resistant allyl cyanoacrylate adhesive. This modified probehead, used in conjunction with the pressurizable Vespel/FEP sample vessel, gave the completely flat spectral base lines needed for accurate spectral integrations.

The pulse cycling time (equal to acquisition time plus delay intervals) was chosen to be greater than the maximum measured[22] $5T_1$ for those samples for which accurate spectral integration was desired. Temperature calibrations for each combination of spectrometer, probehead, and

(2) Freund, E. *Bull. Soc. Chim. Fr.* **1973**, 2238, 2244.
(3) Dutta, P. K.; Shieh, D. C. *Zeolites* **1985**, *5*, 135; *J. Raman Spectrosc.* **1985**, *16*, 312.
(4) Thilo, E.; Wieker, W.; Stade, H. *Z. Anorg. Allg. Chem.* **1965**, *340*, 261.
(5) Hoebbel, D.; Wieker, W. *Z. Anorg. Allg. Chem.* **1973**, *400*, 148.
(6) Lentz, C. W. *Inorg. Chem.* **1964**, *3*, 574.
(7) Dent Glasser, L. S.; Sharma, S. K. *Br. Polym. J.* **1974**, *6*, 283.
(8) Dent Glasser, L. S.; Lachowski, E. E.; Cameron, G. G. *J. Appl. Chem. Biotechnol.* **1977**, *27*, 39. Dent Glasser, L. S.; Lachowski, E. E. *J. Chem. Soc., Dalton Trans.* **1980**, 393, 399.
(9) Ray, N. H.; Plaisted, R. J. *J. Chem. Soc., Dalton Trans.* **1983**, 475.
(10) Marsmann, H. C. *Chem.-Ztg.* **1973**, *97*, 128. Gould, R. O.; Lowe, B. M.; MacGilp, N. A. *J. Chem. Soc., Chem. Commun.* **1974**, 720. Marsmann, H. C. *Z. Naturforsch.* **1974**, *29B*, 495.
(11) Engelhardt, G.; Jancke, H.; Hoebbel, D.; Wieker, W. *Z. Chem.* **1974**, *14*, 109.
(12) Harris, R. K.; Newman, R. H. *J. Chem. Soc., Faraday Trans. 2* **1977**, *73*, 1204.
(13) Harris, R. K.; Jones, J.; Knight, C. T. G.; Pawson, D. *J. Mol. Struct.* **1980**, *69*, 95.
(14) Harris, R. K.; Knight, C. T. G.; Hull, W. G. *J. Am. Chem. Soc.* **1981**, *103*, 1577. Harris, R. K.; Knight, C. T. G. *J. Mol. Struct.* **1982**, *78*, 273; *J. Chem. Soc., Faraday Trans. 2* **1983**, *79*, 1525, 1539.
(15) Kinrade, S. D.; Swaddle, T. W. *J. Chem. Soc., Chem. Commun.* **1986**, 120.
(16) Engelhardt, G.; Hoebbel, D. *J. Chem. Soc., Chem. Commun.* **1984**, 514.
(17) Creswell, C. J.; Harris, R. K.; Jageland, P. T. *J. Chem. Soc., Chem. Commun.* **1984**, 1261.
(18) Kinrade, S. D.; Swaddle, T. W., *Inorg. Chem.*, following paper in this issue.
(19) Since the solutions studied in this work were prepared from SiO_2, MOH, and water opnly, their compositions are conveniently specified as the ratio of concentration of M^+ to total dissolved Si^{IV}. The free OH^- concentration will be less than $[M^+]$ but is not easily specified because of the variable degrees of protonation of the silicate species.
(20) (a) Sjöberg, S.; Öhman, L.-O.; Ingri, N. *Acta Chem. Scand., Ser. A* **1985**, *A39*, 93. (b) Svensson, I. L.; Sjöberg, S.; Öhman, L.-O. *J. Chem. Soc., Faraday Trans. 1* **1986**, *82*, 3635.
(21) (a) Engelhardt, G.; Zeigan, D.; Jancke, H.; Hoebbel, D.; Wieker, W. *Z. Anorg. Allg. Chem.* **1975**, *418*, 17. (b) McCormick, A. V.; Bell, A. T.; Radke, C. J. *Stud. Surf. Sci. Catal.* **1986**, *28*, 247; *Zeolites* **1987**, *7*, 183.
(22) Kinrade, S. D.; Swaddle, T. W. *J. Am. Chem. Soc.* **1986**, *108*, 7159.
(23) Kinrade, S. D.; Swaddle, T. W. *J. Magn. Reson.* **1988**, *77*, 569.

Table I. Correlation between Relative Positions of Selected ^{29}Si Lines and Structural Factors

				rings containing the Si nucleus		adjoining SiO_4 tetrahedra		
line[a]	species[a]	connectivity	δ^b/ppm	3-ring	4-ring	Q^1	Q^2	Q^3
0	I (Q^0)	Q^0	0					
3	IV	Q^1	−8.2					1
4	III ($Q^1Q^2Q^1$)		−8.2				1	
6	II ($Q^1{}_2$)		−8.7			1		
7	VIII	Q^2	−9.8	1				2
8	IV		−9.8	1			1	1
10	V ($Q^2{}_3$)		−10.2	1			2	
13	VI		−14.2		2			2
14	XVIII		−14.5		2			2
20	X ($Q^2{}_4$)		−16.3		1		2	
25	III ($Q^1Q^2Q^1$)		−16.6			2		
27	XI ($Q^3{}_6$)	Q^3	−17.0	1	2			3
28	IX		−17.7	1	2		1	2
36	XVIII		−21.3		3		1	2
37	VI		−22.0		3		3	
43	($Q^3{}_z$)[c]		−25.4					3
46	XVII ($Q^3{}_8$)		−26.7		3			3

[a] Numbered as in ref 14. [b] Typical approximate chemical shifts, relative to Q^0 (dependent on conditions—here, $Na^+:Si^{IV}$ = 1.0:1, $[Si^{IV}]$ = 1.8 mol kg^{-1}, 95 atom % ^{29}Si, −3.8 °C). [c] Identified in this report as the tetrahedral tetramer ($Q^3{}_4$).

sample tube were obtained from the ^1H spectrum of neat ethylene glycol[24] (Fisher, ACS Certified). Sample spinning affected the temperature ±2 K, and air pressure and the sample spinning rate (20 Hz) were kept constant throughout all experiments. Solution temperatures varied by no more than 0.5 K over each run.

The temperature dependences of the ^{29}Si chemical shifts were recorded relative to ^2H. The "absolute" temperature dependence of the ^2H frequency ν^D was determined directly, with the spectrometer in the unlocked mode; this was possible because of the excellent field stability (field divergence <0.01 ppm over 12 h) of the XL-200 superconducting magnet. When the ^{29}Si transmitter frequency ν_{RF} is locked to the characterized ^2H signal, the frequency shift $\Delta\nu_{Si}$ arising from a change in temperature T from T_A to T_B is given by

$$\Delta\nu_{Si} = [(R_B - R_A) - (\nu^D{}_B - \nu^D{}_A)]/\nu_{RF} \quad (1)$$

where $R = \nu_{RF} - \nu_{signal}$.

Results

Chemical Shifts. The ^{29}Si chemical shift information reported here was derived from spectra of silicate solutions having $M:Si^{IV}$ = 4:1 with a natural abundance of ^{29}Si, and $M:Si^{IV}$ = 1.0:1 with either natural-abundance or 95 atom % ^{29}Si. Isotopic enrichment gives enhanced signal-to-noise ratios but leads to line splitting[13,14] and was useful in the present study primarily in obtaining spectral integrations for *groups* of peaks Q^y, as in Figure 1. These groups correspond to silicon centers of connectivities y, i.e., a ^{29}Si nucleus resonates at progressively lower frequencies as the number y of links (through oxygen atoms) to other Si atoms increases. The Q^2 and Q^3 groups can be conveniently subdivided into A and B regions (Figure 1). The assignments of Harris and Knight[14] are used, and the qualitative effects of molecular structure and solution conditions on the chemical shifts $\Delta\delta$ relative to the unique Q^0 resonance are summarized in Tables I and II. At −3.8 °C, the Q^0 resonance lies at δ = −71.3 ppm relative to tetramethylsilane (TMS) for a sample with $[Si^{IV}]$ = 1.75 mol kg^{-1} and $M^+:Si^{IV}$ = 1.0:1, but since δ was also temperature- and concentration-dependent and required the use of special TMS inserts, the $\Delta\delta$ scale was used for convenience. Results are presented here graphically and are summarized qualitatively in Table II; detailed tables of numerical data are available as supplementary material. In accordance with established practice, the symbol $Q^y{}_z$ designates a silicate species consisting exclusively of z interconnected Q^y units.

Effect of pH. As the alkalinity was increased, all ^{29}Si resonances moved up-frequency (downfield), as noted in previous studies.[14,20,21]

Table II. Factors Affecting ^{29}Si Chemical Shifts

factor increased	result	nuclei most affected
	Structure	
local connectivity	shielding (up to 40 ppm)	high local connectivity
occurrence in ring units	deshielding (up to 8.5 ppm)	in 3-ring
adjacent connectivity	deshielding (up to 1 ppm)	high adjacent connectivity
	Solution Conditions	
[MOH]:[Si^{IV}]	deshielding (up to 2.3 ppm[b])	in least strained species
[Si^{IV}][a]	deshielding (up to 0.3 ppm kg mol^{-1})	
atomic mass of M^+	shielding (up to 1.8 ppm[c])	
% ^2H enrichment	deshielding (up to 0.15 ppm[d])	
% ^{29}Si enrichment	see Table III	in most rigid species
temp	deshielding (up to 0.022 ppm K^{-1})	in least rigid species

[a] [MOH]:[Si^{IV}] ratio constant. [b] [MOH]:[Si^{IV}] from 1.0:1 to 4.0:1. [c] M from Na to Rb. [d] Percentage of ^2H (solvent) from 74 to 99%. [e] Percentage of ^{29}Si from 4.7 to 95.1%, at −4 °C.

For example, an increase in the $Na^+:Si^{IV}$ ratio from 1:1 to 4:1 in samples that were otherwise identical caused the monomer (Q^0) resonance to move 0.4 ppm up-frequency relative to the transmitter signal, while all other resonances advanced up-frequency toward the monomer peak. The order of up-frequency shifts was $Q^0 < Q^2{}_3 < Q^1{}_2$.

Temperature Effects. As the temperature was raised, the ^2H signals moved up-frequency at about 0.11–0.12 Hz K^{-1}, and this information was used to determine the temperature dependences of the ^{29}Si resonances. All ^{29}Si signals moved up-frequency with rising temperature, as in Figure 2, with the relative order of line displacement $Q^3{}_4 < Q^3{}_6 < Q^3{}_8 < Q^0 \leq Q^2{}_3 < Q^1{}_2 <$ (Q^2 in $Q^1Q^2Q^1$); lines in the Q^1 and $Q^2{}_B$ regions moved toward the Q^0 signal, while $Q^2{}_A$ and all Q^3 resonances moved away from it; i.e., the separation between the Q^1 and Q^2 groups and between the Q^2 and Q^3 groups became more distinct as the temperature increased (Figure 3).

Effect of [Si]. Figure 4 exemplifies the dependence of the ^{29}Si chemcial shift on the Si concentration; again, the separation

(24) Ammann, C.; Meier, P.; Merbach, A. E. *J. Magn. Reson.* **1982**, *46*, 319.

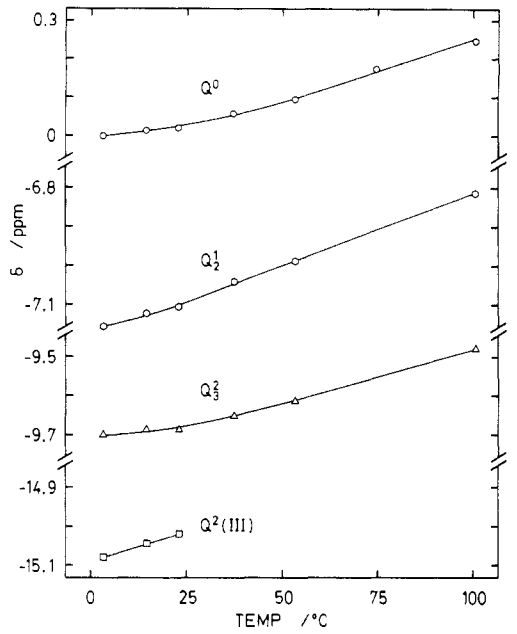

Figure 2. Temperature dependence of all ^{29}Si resonances with $[Si^{IV}]$ = 2.17 mol kg^{-1} and $K^+:Si^{IV}$ = 4.0:1. Signals are referred to the Q^0 resonance at 3.3 °C. Q^2(III) refers to the central Si atom in the acyclic trimer (species III, $Q^1Q^2Q^1$).

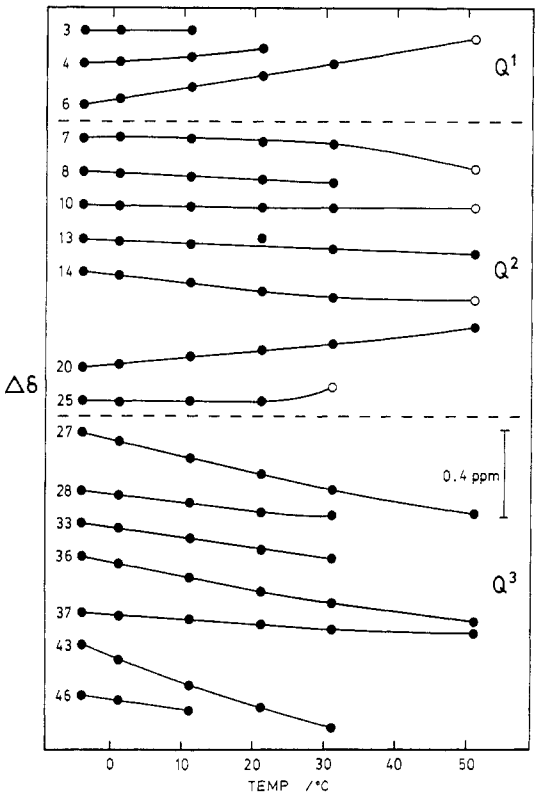

Figure 3. Temperature dependence of ^{29}Si line positions (indexed as in ref 14 and Table I) relative to the Q^0 signal for a sample that contained 1.40 mol kg^{-1} Si with $Na^+:Si^{IV}$ = 1.0:1. The *separations* of the designated lines are not represented to scale. Open symbols signify tentative assignments.

between Q^y groups became clearer as $[Si^{IV}]$ increased.

Effect of M^+. The ^{29}Si resonances were observed at progressively lower frequencies as the alkali-metal cation M^+ was changed from Na^+ to K^+ to Rb^+, as shown for the Q^0 signal in Figure 5. The relative order of line displacement is $Q^0 \leq Q^2{}_3 < Q^1{}_2 \leq (Q^2$ in $Q^1Q^2Q^1)$. Figure 5 also shows that the temperature dependence of shifts is greater for M = Na than for M = K or Rb.

Isotope Effects. An increase in the isotopic concentration of ^2H from the usual 75% to 99% caused minor up-frequency shifts

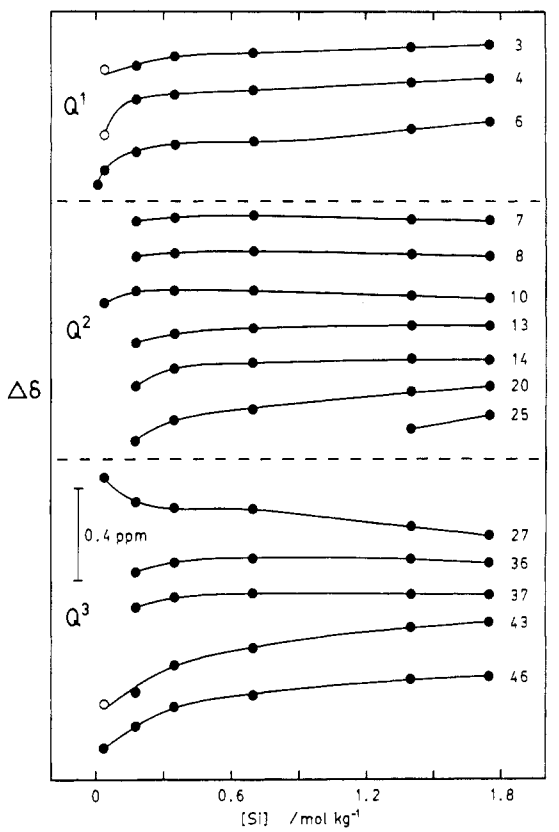

Figure 4. Si^{IV} concentration dependence of ^{29}Si line positions (indexed as in ref 14) at 11.2 °C relative to the Q^0 signal for samples with $Na^+:Si^{IV}$ = 1.0:1. The *separations* of the designated lines are not represented to scale.

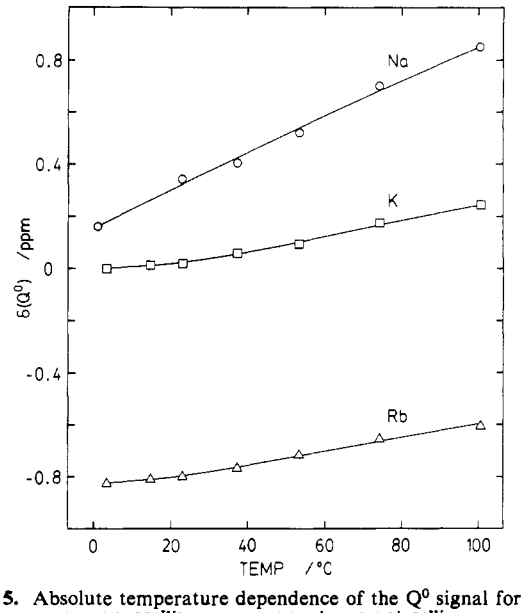

Figure 5. Absolute temperature dependence of the Q^0 signal for M = K, Na, and Rb, with $[Si^{IV}]$ = 2.2 mol kg^{-1} and $M^+:Si^{IV}$ = 4.0:1 in all cases. Signals are referred to the Q^0 position for M = K at 3.3 °C.

of all lines, in the order $Q^0 < Q^2{}_3 < Q^1{}_2 < (Q^2$ in $Q^1Q^2Q^1)$. An increase in the ^{29}Si abundance from 4.7% (natural) to 95.1% resulted in various small up-frequency shifts for most resonances, especially at low temperatures. This is illustrated for a particular solution in Table III, in which the two-bond isotope effect parameter $^2\Delta Si(^{29}Si)$ is defined as in Hansen's review,[25] i.e., as the change in $\Delta\delta$ on going from 95 atom % ^{29}Si to 95 atom % ^{28}Si.

Equilibria. It was found, in confirmation of previous reports,[15,21] that the proportion of resonances which correspond to centers of

(25) Hansen, P. E. *Annu. Rep. NMR Spectrosc.* **1983**, *15*, 105.

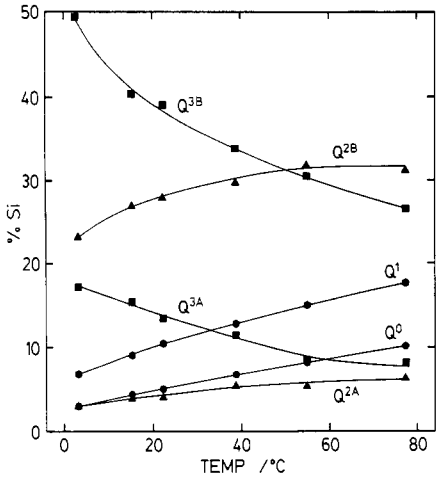

Figure 6. Temperature dependence of integrated spectral band intensities for $[Si^{IV}] = 0.80$ mol kg^{-1} and $Na^+:Si^{IV} = 1.0:1$.

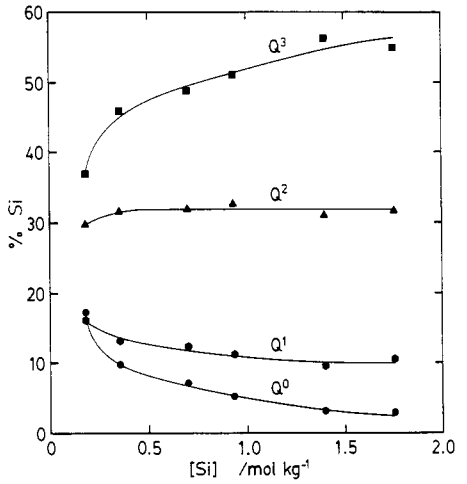

Figure 7. Si^{IV} concentration dependence of integrated spectral band intensities at 21.2 °C for $Na^+:Si^{IV} = 1.0:1$.

high connectivity decreases sharply as the $M^+:Si^{IV}$ ratio is raised above 1:1. Hence, increased alkalinity causes silicate ions to depolymerize. Unfortunately, the integration of individual peak areas is rarely possible because of signal overlap, the large number of resonances, temperature-dependent line broadening,[15-18] and (in ^{29}Si-enriched samples) Si–Si coupling. Nevertheless, the gross features of the equilibrium distribution of silicate ions can be monitored in terms of the six spectral regions defined in Figure 1.

Figure 6 shows that condensation equilibria shift in favor of the monomer and species of low molar mass as the temperature is increased. Despite the significant structural differences represented by the wide frequency separation, the temperature dependences of the Q^2_A and Q^2_B integrations are similar, as for the Q^3_A and Q^3_B groups. Figure 7 shows that depolymerization is favored by sample dilution, as expected, so that, at 0.01 mol kg^{-1} of Si, only the monomer and a small amount (<5%) of the dimer Q^1_2 could be detected even with an $M^+:Si^{IV}$ ratio of 1.0:1.

In general, the concentration and identity of M^+ did not have an important effect on the distribution of silicate oligomers at any alkalinity, although Figure 8 (for $M^+:Si^{IV} = 4.0:1$) shows that progressive substitution of Na with K and then Rb caused oligomer concentrations to be somewhat enhanced at the expense of the monomer, particularly at low temperatures, and (at $M^+:Si^{IV} = 1.5:1$) lines assigned to the Q^3_6 and Q^3_8 species grew in intensity. The degree of deuterium enrichment of the solutions had no discernible effect on the degree of polymerization.

Table III. ^{29}Si Isotope Effects on ^{29}Si Chemical Shifts[a]

		$^2\Delta Si(^{29}Si)$/ppm		
line[b]	resonating nucleus[b]	3.3 °C	22.4 °C	38.8 °C
6	Q^1 in III[c]	−0.03	−0.04	−0.03
10	Q^2 in V[d]	0.00	+0.01	+0.01
13	Q^2 in VI[e]	+0.13	+0.07	+0.03
14	Q^2 in XVIII[f]	+0.22	+0.12	+0.05
27	Q^3 in XI[g]	+0.21	+0.14	+0.04
36	Q^3 in XVIII[f]	+0.20	+0.12	+0.05
37	Q^3 in VI[e]	+0.15	+0.08	+0.02
43	Q^3 in Q^3_4	+0.19	+0.08	+0.02

[a] Conditions: $[Si^{IV}] = 2.2$ mol kg^{-1}; $M^+:Si^{IV} = 1.0:1$; $^2\Delta Si(Si^{29})$ = ($\Delta\delta$ for 4.7 atom % ^{29}Si) − ($\Delta\delta$ for 95.1 atom % ^{29}Si). [b] Nomenclature of ref 14. [c] Dimer. [d] Cyclic trimer. [e] Singly bridged 4-ring. [f] Doubly bridged 4-ring. [g] Double 3-ring (hexagonal prism).

Discussion

Chemical Shifts. Structural Effects. The most important factor influencing ^{29}Si shifts is the local degree y of silicate connectivity, which is responsible for the basic separation of 8.5 ppm between the major Q^y groups.[12-14] The next most prominent shielding influence shown by Table I is the presence of the resonating nucleus in a cyclic unit, which causes an up-frequency shift from the basic 8.5 ppm spacing pattern, to the extent that it is convenient to subdivide the Q^2 and Q^3 resonances into A (up-frequency) and B subregions. For example, Q^2 nuclei in a 4-ring resonate at slightly higher frequencies than the Q^2 signal of the acyclic trimer, while those occurring simultaneously in *two* 4-rings are shifted further up-frequency, though still within the Q^2_B subregion; Q^2 nuclei in 3-rings, however, are shifted strongly upfrequency, into the Q^2_A subregion. A similar trend is apparent for the Q^3 resonances. Theoretical calculations[26] show that 3-rings are more

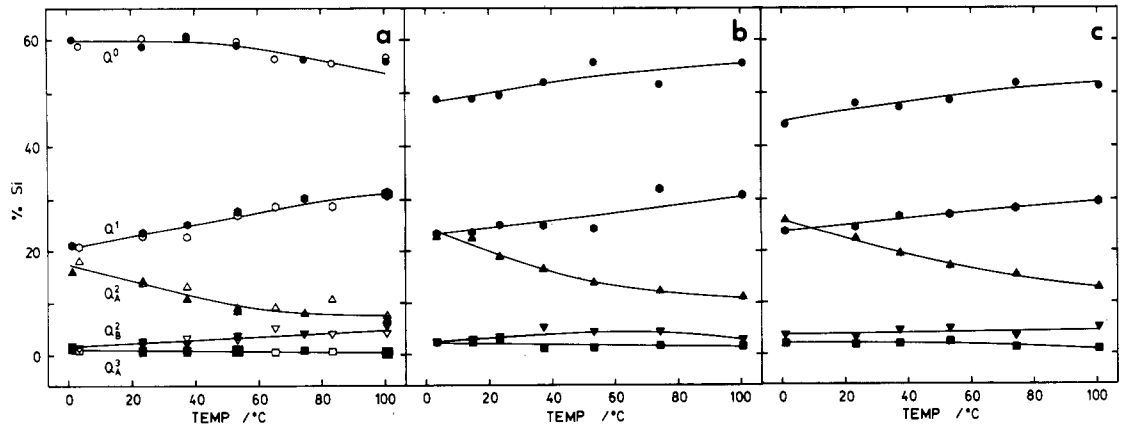

Figure 8. Temperature dependence of integrated spectral band intensities: (a) M = Na (open symbols, 99% ^{2}H enrichment; filled symbols, 75% ^{2}H); (b) M = K; (c) M = Rb. All samples contained 2.2 mol kg^{-1} Si with $M^+:Si^{IV} = 4.0:1$.

strained than 4-rings, which in turn are generally more strained than acyclic silicate species, and that the longer Si–O bonds and smaller Si–O–Si bond angles associated with strain will be associated with less efficient Si–O σ (and π) orbital overlap and hence with enhanced deshielding.

In Table I, the relative positions of lines 3–6, 7–10, and 19–25 indicate that shielding is further reduced by high connectivity at *adjoining* SiO_4 tetrahedra. Molecular models show that silicate ligands which are themselves of high connectivity are bulky and increase molecular strain.

Effect of pH. At high alkalinity, deprotonation of Si–OH groups will increase the deshielding of the Si, and this will be an important factor contributing to the dependence of the chemical shift on the M^+:Si^{IV} ratio.[14,20,21] Unfortunately, line shifts cannot be used to determine the relative acidities of the various Si–OH groups because deprotonation cannot be isolated from other shielding influences affected by the M^+:Si^{IV} ratio, such as M^+–silicate ion pairing.

Isotope Effects. Although the usual additivity of isotope effects[25] might be expected to lead to a strong correlation between $^2\Delta Si(^{29}Si)$ and connectivity at the resonating Si nucleus, Table III suggests that $^2\Delta Si(^{29}Si)$ is controlled mainly by the influences of Si–O–Si strain (see below)[26,27] and framework rigidity upon molecular vibrations.[25] Table III also highlights the marked temperature dependence of the Si isotope effect, which follows the normal pattern and is therefore also attributable to vibrational phenomena.[25]

Concentration and Counterion Effects. Changes in solution composition affected ^{29}Si shielding to an extent sometimes approaching that of minor structural differences. Increases in the Si^{IV} concentration led to small up-frequency shifts (Table II). The order of line displacement $Q^3_6 \leq Q^2_3 < Q^1_2 \simeq (Q^2$ in $Q^1Q^2Q^1) < Q^3_8 \approx Q^2_4 < Q^3_4$ (Figure 4) correlates inversely with the predicted molecular strain (smallness of Si–O–Si bond angles).[26,27] The fact that $\Delta\delta$ also depends on the M^+ concentration at a fixed M^+:Si^{IV} ratio, and on the identity of M, shows that there is a significant shielding contribution from silicate–M^+ interactions and that this varies between different Si centers. It might be expected that this cation effect reflects a trend in the M^+–silicate ion-pair formation constants K_{IP}; crude Fuoss-type calculations[22,28] show that the variation of K_{IP} with M^+ should be unimportant for the monomer $H_3SiO_4^-$ but appreciable effects of M^+ on K_{IP} may occur with the larger, multiply charged oligomers (cf. discussion of equilibria below).

Structural Information from Chemical Shift Data. The patterns of relative line shifts established above can be used to identify new species and to support tentative assignments of resonances. In particular, resonances assigned by Harris and Knight[14] to the tentative structures VII and XII–XVI do indeed behave as expected. A new assignment can also be made; the line starred in Figure 1 (line 43 of Harris et al.[14]) is an unsplit resonance situated in the Q^3_B region at $\Delta\delta \approx -25.4$ ppm and therefore corresponds to a completely symmetrical silicate anion containing z magnetically equivalent Q_3 centers (Q^3_z). Although this resonance was formerly attributed to the Q^3_8 species,[14] it is currently unassigned. Of all the resonances monitored, this line was displaced least up-frequency as the temperature was raised but most up-frequency with increasing silicate concentration (Figures 3 and 4, line 43), and the shift patterns of Table II therefore indicate that it corresponds to an unusually strain-free but rigid molecule. Symmetrical structures Q^3_z with $z = 6$ and 8 are already accounted for, those with $z = 1$, 2, 3, 5, 7, and 9 are not possible, ball and stick models indicate that structures with $z = 10$ or more are quite flexible and, because of O···O interactions, strained as well, and the strained double-5-ring species Q^3_{10} has been tentatively associated with a resonance at −26.5 ppm[29] but is known only in solutions containing tetrapropylammonium ions and dimethyl sulfoxide.

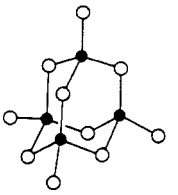

Figure 9. Proposed structure of the species giving rise to the starred line of Figure 1.

These considerations leave little doubt that the starred line corresponds to the species Q^3_4 (Figure 9), in which the Si atoms are deployed at the vertices of a regular tetrahedron and the adamantane-like Si–O framework maintains the unstrained O–Si–O angle of the orthosilicate ion with maximum separation between $-O^-$ groups. Under the conditions of these experiments (M^+:Si^{IV} = 1.0 or more), there will be one or more negative charges per Si in any silicate species,[20] so that the Q^3_4 entity is $Si_4O_{10}^{4-}$. This structure is presently unknown in any solid silicate phase, although the structurally analogous organosilsesquioxanes $(RSiO_{1.5})_4$, in which R is $(CH_3)_2CH-$ or $(CH_3)_3C-$, have been known since 1955[30] and the silane $H_4Si_4S_6$, which also has the adamantane-like framework, has recently been synthesized and found to be very stable.[31] The $Si_4O_{10}^{4-}$ ion is isoelectronic and presumably isostructural with P_4O_{10}.

Silicate Equilibria. Although the complexity of ^{29}Si NMR spectra in aqueous silicates precludes the determination of equilibrium constants for the formation of particular molecular species, it has proved possible to show, by following changes in the populations of the connectivity groups defined in Figure 1, that condensation of silicate units is favored by low temperatures, low alkalinities, and high concentrations of Si^{IV}. These results form a necessary background for the study of the kinetics and mechanism of silicate condensation.[18] Ray and Plaisted[9] also reported that the degree of polymerization in aqueous silicates increased with Si^{IV} concentration and decreased with rising temperature or M^+:Si^{IV} ratio, but their studies involved solutions with M^+:Si^{IV} ratios ranging from 0.05 up to 1.0 (i.e., with colloidal silica present) and used the trimethylsilylation technique, which, as noted above, may not give a faithful picture of speciation in a labile silicate system.

The dependence of the condensation equilibria on the alkali-metal cation has not previously been observed by NMR, although the trimethylsilylation studies of Ray and Plaisted[9] showed that the degree of polymerization tended to increase with increasing ionic radius of M^+, in accordance with the present findings. Dutta and Shieh[3] could find no difference between Raman spectra of silicate solutions prepared with M^+ = Li, Na, K, or Rb. The preferential stabilization of the larger oligomers by the heavier M^+ may reflect larger ion-pair formation constants K_{IP}; calculated values of K_{IP} for the orthosilicate *monomer* showed no significant dependence on M^+,[22] but the effects noted above of M^+ on chemical shifts suggest that K_{IP} may indeed increase from M = Na to K to Rb, the increase being small for the monomer but significant for the higher oligomers. In support of this view, we note that K_{IP} values for the pairing of vanadate ions with M^+ decreases from M = Na to M = K for the monomer HVO_4^{2-} whereas K_{IP} values for the $V_{10}O_{28}^{6-}$–M^+ pairs are comparatively large and increase from Na to K to Rb.[32] The influence, albeit small, that alkali-metal ions exert over the distribution of silicate polymers in aqueous solution may provide some insight into the effects they are thought to have over the size and shape of silicate

(26) Chakoumakos, B. C.; Hill, R. J.; Gibbs, G. V. *Am. Mineral.* **1981**, *66*, 1237.
(27) Janes, N.; Oldfield, E. *J. Am. Chem. Soc.* **1985**, *107*, 6769; **1986**, *108*, 5743.
(28) Fuoss, R. M. *J. Am. Chem. Soc.* **1958**, *80*, 5059.
(29) Boxhoorn, G.; Sudmeijer, O.; Van Kasteren, P., H. G. *J. Chem. Soc., Chem. Commun.* **1983**, 1416.
(30) Wiberg, E.; Simmler, W. *Z. Anorg. Allg. Chem.* **1955**, *282*, 330; **1956**, *283*, 26. Schwab, G. M.; Grabmaier, J.; Simmler, W. *Z. Phys. Chem. (Munich)* **1956**, *6*, 376.
(31) Haas, A.; Hitze, R.; Krueger, C.; Angermund, K. *Z. Naturforsch.* **1984**, *39B*, 890.
(32) Schwarzenbach, G.; Geier, G. *Helv. Chim. Acta* **1963**, *46*, 906.

units in the formation of minerals.[33,34]

Finally, it is significant that, with the care taken to eliminate all sources of silicon other than the solution samples themselves from the probehead, the ^{29}Si spectra of all the silicate solutions examined were completely blank, with zero intergrated intensity, in the Q^4 region (ca. −30 ppm and beyond, relative to the Q^0 resonance). Harris and co-workers,[35] in a two-dimensional ^{29}Si NMR study of aqueous silicates, were similarly unable to detect any sharp peaks in the Q^4 region, although Svensson et al.[20b] reported evidence for Q^4 centers in aged silicate solutions (decanted from a precipitate) with $Na^+:Si^{IV} < 1.0:1$, in which colloidal or suspended silica would be expected to be present. Evidently, the connectivity of silicate centers cannot exceed 3 in true solution in water, although colloidal silica or silicates, if present, may contain Q^4 centers.

Acknowledgment. We thank the Alberta Oil Sands Technology and Research Authority for a scholarship (to S.D.K.) and the University of Calgary Research Grants Committee and the Natural Sciences and Engineering Research Council of Canada for financial assistance.

Supplementary Material Available: Tables of solution compositions, ^{29}Si shifts as functions of temperature and solution composition, and spectral integration data for aqueous alkaline silicate solutions (10 pages). Ordering information is given on any current masthead page.

(33) Barrer, R. M. *Hydrothermal Chemistry of Zeolites*; Academic: London, 1982.
(34) Iler, R. K. *The Chemistry of Silica*; Wiley: New York, 1979.
(35) Harris, R. K.; O'Connor, M. J.; Curzon, E. H.; Howarth, O. W. *J. Magn. Reson.* **1984**, *57*, 115.

Contribution from the Department of Chemistry, The University of Calgary, Calgary, Alberta, Canada T2N 1N4

Silicon-29 NMR Studies of Aqueous Silicate Solutions. 2. Transverse ^{29}Si Relaxation and the Kinetics and Mechanism of Silicate Polymerization

Stephen D. Kinrade† and Thomas W. Swaddle*

Received November 25, 1987

For solutions of SiO_2 in aqueous MOH (M = Na, K, Rb) with $M^+:Si^{IV} = 1:1$ (in which each Si carries one $-O^-$ group), the temperature-dependent ^{29}Si line broadening is almost entirely due to Si–Si chemical exchange, if contaminants are absent, and is uniform for most resonances. This implies involvement of a common vehicle of intermolecular Si exchange (polymerization)—evidently the neutral form of the monomer, $Si(OH)_4$. The temperature dependence of the inverse spin-site lifetime τ^{-1} is given by $\Delta H^* = 50$ kJ mol^{-1} and $\Delta S^* = -69$ J K^{-1} mol^{-1}. Intramolecular cyclization processes are faster than intermolecular polymerization and result in greater line broadening for a few minor peaks. For solutions with $M^+:Si^{IV} > 1:1$ (high pH), silicate species that have more than one $-O^-$ per Si and that are relatively unreactive in Si–Si exchange form to varying degrees, leading to reduced and nonuniform temperature-dependent line broadening. When this is taken into account, Si–Si chemical exchange is seen to explain both ^{29}Si line broadening and the results of selective inversion-recovery experiments.

Introduction

We have remarked[1,2] that the use of ^{29}Si NMR for the characterization of hydrothermal silicate solutions is limited by the marked broadening of the spectral lines as the temperature is increased. Engelhardt and Hoebbel[3] suggested that this broadening was due to chemical exchange of SiO_4 units between the silicate anions at rates within the NMR time frame. Although Harris and co-workers originally put forward a similar suggestion,[4] they later reported[5] spin saturation-transfer experiments that implied exchange rates some 2 orders of magnitude lower than had been estimated from line-width measurements. They noted that line broadening was particularly severe (and not completely reversible) when the samples were heated in the spectrometer in unlined glass NMR tubes[4] and concluded that paramagnetic contaminants introduced during sample preparation and/or by leaching from glass NMR tubes were the most likely cause of both longitudinal relaxation (time constant T_1) and line broadening (transverse relaxation T_2).[5] Both research groups reported that the extent of temperature-dependent line broadening varied from resonance to resonance.[3,4]

Griffiths, Cundy, and Plaisted[6] recently employed the Carr–Purcell–Meiboom–Gill pulse sequence[7] in an attempt to quantify the contribution of Si–Si exchange to ^{29}Si line widths in aqueous silicates. Their conclusions, however, are based upon limited data and are not unequivocal, since unlined glass NMR tubes were used and the possible effect of pseudo-T_2 relaxation arising from field inhomogeneities was not taken into account. Thus, while NMR methods afford unique insights into the complicated aqueous chemistry of silicates, definitive results have been elusive and are likely to remain so.

The present paper reports a detailed study of ^{29}Si line broadening in silicates as a function of temperature (up to 144 °C) and solution composition (expressed as the total concentration $[Si^{IV}]$ of silica dissolved in aqueous MOH, where M is an alkali-metal ion, and the concentration ratio $M^+:Si^{IV}$[1]), with special attention to the avoidance of contamination of the solutions; an ancillary study[8] of longitudinal relaxation in these systems showed that paramagnetic contamination can readily be reduced to insignificance. It will be shown that the temperature-dependent line broadening is indeed due to chemical exchange of silicate units and that this is strongly pH-dependent, which accounts for some of the disagreement in the literature, as was pointed out in a brief preliminary communication.[2] The mechanistic implications will also be considered. Finally, an error in our preliminary communication[2] is corrected.

Experimental Section

The preparation of the solution and the conduct of the NMR experiments are described in the preceding paper.[1] Full details of the sample compositions are given in the supplementary material of ref 1. Several

†Present address: Department of Chemistry, Lakehead University, Thunder Bay, Ontario, Canada P7B 5E1.

(1) Kinrade, S. D.; Swaddle, T. W. *Inorg. Chem.*, preceding paper in this issue.
(2) Kinrade, S. D.; Swaddle, T. W. *J. Chem. Soc., Chem. Commun.* **1986**, 120. The table in this preliminary note should be disregarded.
(3) Engelhardt, G.; Hoebbel, D. *J. Chem. Soc., Chem. Commun.* **1984**, 514.
(4) Harris, R. K.; Jones, J.; Knight, C. T. G.; Newman, R. H. *J. Mol. Liq.* **1984**, *29*, 63.
(5) Creswell, C. J.; Harris, R. K.; Jageland, P. T. *J. Chem. Soc., Chem. Commun.* **1984**, 1261.
(6) Griffiths, L.; Cundy, C. S.; Plaisted, R. J. *J. Chem. Soc., Dalton Trans.* **1986**, 2265.
(7) Farrar, T. C.; Becker, E. D. *Pulse and Fourier Transform NMR*; Academic: New York, 1971; p 104.
(8) Kinrade, S. D.; Swaddle, T. W. *J. Am. Chem. Soc.* **1986**, *108*, 7159.

0020-1669/88/1327-4259$01.50/0